ELSEVIER

A study of absorption enhancement by wavy film flows

Vikas Patnaik and Horacio Perez-Blanco
Department of Mechanical Engineering, The Pennsylvania State University, University Park, PA, USA

The mass transfer rates into wavy falling films are larger than those predicted by smooth-film theory. Inertial, roll waves in the falling film flowing over a vertical tube are responsible for the largest enhancement. Transient, two-dimensional (2-D) governing equations were formulated for simultaneous heat and mass transfer in the film, with roll wave hydrodynamics as input. The equations, coupled nonlinearly at the vapor–liquid interface, were solved by an iterative finite-difference scheme. Average heat and mass transfer coefficients were extracted from the results and compared to experimental as well as theoretical data from the literature. Excellent agreement with penetration theory was obtained for the smooth film, but in the roll wave regime, the model predicted much higher transport rates than those possible with a smooth film. The model results indicate that the normal convective flux attributable to the transverse velocity in its inward phase, coupled with the effect of the corresponding streamwise velocity, is responsible for transport enhancement in such wavy films.

Introduction

Absorption technology is becoming increasingly competitive with vapor compression technology, in light of the environmentally friendlier working fluids and thermal activation. The absorber performance largely defines the cycle performance. In the absorber, refrigerant vapor from the evaporator is absorbed into an absorbent liquid. A large heat of mixing is usually released as a result of this, which has to be convected away to maintain the driving force for the absorption. The modeling of this process plays a crucial role in the design and performance prediction of absorption cooling and heating machines and other related equipment.

The vertical tube absorber has found application in some industrial and commercial chilling machines and is used as a research tool to study falling film absorption. The vertical tube configuration lends itself to a number of enhancement techniques for simultaneous heat and mass transport. The waves arising in the film due to instabilities associated with the transition regime play a key role in enhancing absorption.

Pioneering theoretical work was done by Grigor'eva and Nakoryakov (1977), when they obtained an exact solution to the combined heat and mass transfer problem during falling-film absorption. In their model, they assumed an isothermal wall over which a laminar film of constant thickness flowed and solved for the temperature and concentration fields, neglecting the effect of waves. Andberg and Vliet (1983) developed a model for non-isothermal absorption of water vapor into a laminar film of aqueous lithium bromide solution flowing down a constant temperature vertical flat plate. They solved the problem numerically and presented design guidelines for typical absorption cooling equipment. Grossman (1983) improved the uniform-velocity model used by Grigor'eva and Nakoryakov by assuming a parabolic velocity profile. He also extended the model by including the adiabatic wall case. He found that the Nusselt and Sherwood numbers depended on the Peclet and Lewis numbers, as well as on the equilibrium characteristics of the working fluids.

Habib and Wood (1990) considered both phases in the simultaneous heat and mass transfer in vertical absorbers by including the momentum and energy equations for the gas (vapor) phase, along with interfacial drag, in the problem formulation. Their two-phase cocurrent flow was bounded by an isothermal wall on the liquid side and an adiabatic wall on the vapor side. The results of their numerical solution, based on Patankar's control-volume discretization (1980), indicated that the absorption rate increases greatly with absorber (vapor) pressure, inlet solution concentration, and decreasing isothermal wall temperature. A finite-element method was employed by van der Wekken et al. (1988) to solve the same problem for *steady*, laminar film flow, described hence by elliptic partial differential equations.

All of the above models yielded steady-state solutions for smooth films. The waviness of the falling film has been accounted for in some models, but only under isothermal conditions. Beschkov and Boyadjiev (1983) considered such mass transfer to be an "elliptic" phenomenon by retaining the species diffusion term in the streamwise direction and adopting the hydrodynamics of Penev et al. (1972) to describe the wavy flow. Wasden and Dukler (1990) also simulated isothermal mass transfer into falling films. Their numerical analysis assumed the presence of roll waves (Brauner 1989) at the vapor–liquid interface. This work was extremely useful in illustrating the

Address reprint requests to Prof. H. Perez-Blanco, Department of Mechanical Engineering, The Pennsylvania State University, University Park, PA 16802, USA.

Received 20 January 1995; accepted 23 August 1995

655 Avenue of the Americas, New York, NY 10010

0142-727X/96/$15.00
SSDI 0142-727X(95)00076-3

Notation *

A	area
C	concentration, mole/m^3
c_p	specific heat
D_{AB}	liquid diffusion coefficient for binary mixture AB
G_1, G_2	empirical coefficients for wall (coolant) temperature function
I	partial enthalpy
i	enthalpy
k	thermal conductivity
L	absorber tube length
m	mass (flow) rate
N	molar flux
Nu	Nusselt number
p	pressure
$\Pr = \nu/\alpha$	Prandtl number
q, Q	heat rate
r	tube radius
R_r	(chemical) reaction rate
$\mathrm{Re} = 4w\delta/\nu$	Reynolds number
$\mathrm{Sc} = \nu/D_{AB}$	Schmidt number
$\mathrm{Sh} = \kappa\delta/D_{AB}$	Sherwood number
t	time
T	temperature
w	longitudinal velocity
v	transverse velocity
x	concentration, mass fraction
X	concentration, mole fraction
y	transverse coordinate (from outer wall)
z	longitudinal coordinate (from top)

Greek

α	thermal diffusivity
δ	film thickness
ζ	normalized transverse coordinate
κ	mass transfer coefficient
ν	kinematic viscosity
ρ	density
Φ	viscous dissipation

Subscripts

A, B	component A, component B in binary mixture
0	initial conditions
abs	of absorption
c	coolant
eq	equilibrium
fg	(liquid–vapor) phase-change property
FD	fully developed
i	inlet
if	interface
o	outer wall or bulk, time-averaged outlet conditions
r	refrigerant
s	solution (bulk)
v	vapor
w	wall

Superscripts

$-$	averaged quantity or molal property (see context)
	generation per unit volume

transport-enhancing effects of roll waves, but did not describe the thermal effects resulting from absorption involving working pairs that form a nonideal solution.

Nonstationary waves at the falling film surface call for an unsteady, two-dimensional (2-D) approach to modeling (Patnaik 1994). The present work consists of setting up the governing equations and boundary conditions for transient simultaneous heat and mass transfer in the film. The flow regime plays a crucial role in the transport processes within the falling film. Figure 1 illustrates the two types of wavy-laminar flow known to occur: capillary ($20 < \mathrm{Re}_s < 200$) and inertial or roll waves ($200 < \mathrm{Re}_s < 1000$). In the latter type, a large portion of the flow is carried by liquid lumps rolling over a thin substrate film. The substrate can be laminar or itself have capillary waves, but the rolling waves are gravity driven and of low frequency. This is the flow regime of interest to this work. A complete velocity field was formulated obtained for roll waves (Patnaik 1994).

Mathematical model

The analysis is performed based on the following assumptions.

(1) The problem is 2-D in nature; both y (transverse) and z (longitudinal) directions are of interest.
(2) The falling film is laminar or wavy-laminar ($\mathrm{Re}_s < 1000$).
(3) The falling film is much thinner than the outer radius of the absorber tube, i.e.; $\bar{\delta} \ll r_o$ so that curvature effects are neglected.
(4) Constant absorbent thermophysical properties and incompressible flow exist.

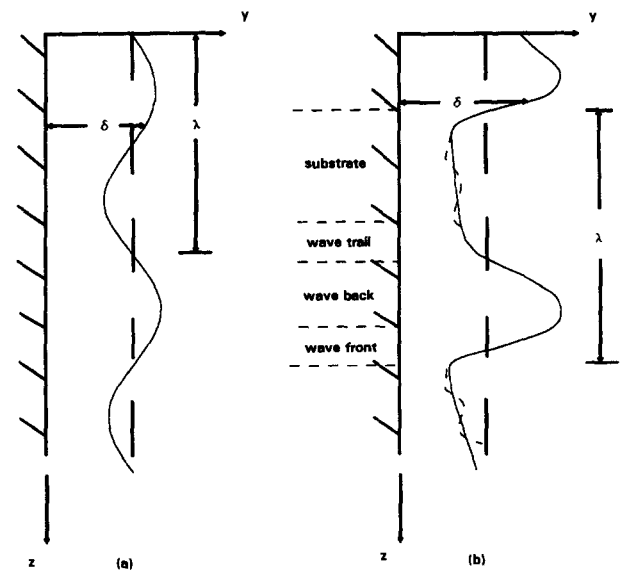

Figure 1 a Capillary waves; b roll waves

* All quantities in S.I. units.

(5) Pressure equilibrium exists at the vapor–liquid interface at all times, according to the vapor pressure data of McNeely (1979) for LiBr–water solutions.
(6) The vapor is still, with uniform pressure and temperature.
(7) There are no noncondensibles (such as air) in the vapor phase, so that there is no resistance to mass transfer in this phase.
(8) The heat transferred from the solution to the vapor is negligible.

The transport of the absorbate in the liquid film is governed by the convective–diffusion equation, which is the result of a mass balance for a differential element of the solution. Expressed in 2-D Cartesian coordinates, we have the general elliptic form (Patankar 1988):

$$\frac{\partial C}{\partial t} + w\frac{\partial C}{\partial z} + v\frac{\partial C}{\partial y} = D_{AB}\left(\frac{\partial^2 C}{\partial z^2} + \frac{\partial^2 C}{\partial y^2}\right) + R_r \tag{1}$$

Under most conditions of film flow, molecular diffusion in the streamwise direction is negligible with respect to that in the transverse direction:

$$\frac{\partial^2 C}{\partial z^2} \ll \frac{\partial^2 C}{\partial y^2}.$$

No chemical reactions take place, so that $R_r = 0$. The convective–diffusion equation then takes the parabolic form:

$$\frac{\partial C}{\partial t} + w\frac{\partial C}{\partial z} + v\frac{\partial C}{\partial y} = D_{AB}\frac{\partial^2 C}{\partial y^2} \tag{2}$$

The energy equation in its general 2-D form is:

$$\rho\frac{\partial i}{\partial t} + \rho w\frac{\partial i}{\partial z} + \rho v\frac{\partial i}{\partial y} = k\left(\frac{\partial^2 T}{\partial z^2} + \frac{\partial^2 T}{\partial y^2}\right) + \left(w\frac{\partial p}{\partial z} + v\frac{\partial p}{\partial y}\right) + \mu\Phi + \dot{q} \tag{3}$$

Viscous dissipation is neglected, because the falling film velocities are small, along with the contribution of pressure-work. Finally, analogous to the case of species concentration,

$$\frac{\partial^2 T}{\partial z^2} \ll \frac{\partial^2 T}{\partial y^2}$$

The energy equation then reduces to the parabolic form:

$$\rho\frac{\partial i}{\partial t} + \rho w\frac{\partial i}{\partial z} + \rho v\frac{\partial i}{\partial y} = k\frac{\partial^2 T}{\partial y^2} + \dot{q} \tag{4}$$

The last term represents the heat generated per unit volume attributable to the diffusion of absorbate into the film, and is given as:

$$\dot{q} = \frac{\partial}{\partial y}\left[D_{AB}\frac{\partial C}{\partial y}\cdot\rho\frac{\partial i}{\partial C}\right]_T \tag{5}$$

for incompressible flow (Grossman and Heath 1984).

The functional relationship $i = i(T, C)$ is readily available for aqueous lithium bromide (McNeely 1979). We can then write:

$$\frac{\partial i}{\partial t} = \left.\frac{\partial i}{\partial T}\right]_C\frac{\partial T}{\partial t} + \left.\frac{\partial i}{\partial C}\right]_T\frac{\partial C}{\partial t} \tag{6}$$

$$\frac{\partial i}{\partial z} = \left.\frac{\partial i}{\partial T}\right]_C\frac{\partial T}{\partial z} + \left.\frac{\partial i}{\partial C}\right]_T\frac{\partial C}{\partial z} \tag{7}$$

$$\frac{\partial i}{\partial y} = \left.\frac{\partial i}{\partial T}\right]_C\frac{\partial T}{\partial y} + \left.\frac{\partial i}{\partial C}\right]_T\frac{\partial C}{\partial y} \tag{8}$$

The quantities $(\partial i/\partial T)_C$ and $(\partial i/\partial C)_T$ represent thermodynamic properties of the absorbent solution. By definition,

$$\left.\frac{\partial i}{\partial T}\right]_C = c_p \quad \text{and} \quad \rho\left.\frac{\partial i}{\partial C}\right]_T = \bar{i} \tag{9}$$

are the specific heat and molal enthalpy, respectively. Substituting the above results in Equation 4, for constant c_p we get:

$$\left(\rho\, c_p\frac{\partial T}{\partial t} + \bar{i}\frac{\partial C}{\partial t}\right) + w\left(\rho\, c_p\frac{\partial T}{\partial z} + \bar{i}\frac{\partial C}{\partial z}\right) + v\left(\rho\, c_p\frac{\partial T}{\partial y} + \bar{i}\frac{\partial C}{\partial y}\right) = k\frac{\partial^2 T}{\partial y^2} + \dot{q} \tag{10}$$

$$\therefore \rho\, c_p\left(\frac{\partial T}{\partial t} + w\frac{\partial T}{\partial z} + v\frac{\partial T}{\partial y}\right) + \bar{i}\left(\frac{\partial C}{\partial t} + w\frac{\partial C}{\partial z} + v\frac{\partial C}{\partial y}\right) = k\frac{\partial^2 T}{\partial y^2} + \dot{q} \tag{11}$$

Substituting from Equations 2 and 5, we get:

$$\rho\, c_p\left(\frac{\partial T}{\partial t} + w\frac{\partial T}{\partial z} + v\frac{\partial T}{\partial y}\right) + \bar{i}\left(D_{AB}\frac{\partial^2 C}{\partial y^2}\right) = k\frac{\partial^2 T}{\partial y^2} + \frac{\partial}{\partial y}\left[D_{AB}\frac{\partial C}{\partial y}\bar{i}\right] \tag{12}$$

Now, the last term can be written as:

$$\frac{\partial}{\partial y}\left[D_{AB}\frac{\partial C}{\partial y}\bar{i}\right] = \bar{i}\frac{\partial}{\partial y}\left[D_{AB}\frac{\partial C}{\partial y}\right] + D_{AB}\frac{\partial C}{\partial y}\frac{\partial}{\partial y}[\bar{i}] \tag{13}$$

For constant molecular diffusivity, the first term on the right-hand side is identical to the last term on the left-hand side of equation 12, thereby cancelling each other out in that equation to give:

$$\rho\, c_p\left(\frac{\partial T}{\partial t} + w\frac{\partial T}{\partial z} + v\frac{\partial T}{\partial y}\right) = k\frac{\partial^2 T}{\partial y^2} + D_{AB}\frac{\partial C}{\partial y}\frac{\partial}{\partial y}[\bar{i}] \tag{14}$$

For moderate changes in temperature and concentration, the molal enthalpy can be treated as a constant thermophysical property. Hence, the energy equation takes the following form:

$$\rho\, c_p\left(\frac{\partial T}{\partial t} + w\frac{\partial T}{\partial z} + v\frac{\partial T}{\partial y}\right) = k\frac{\partial^2 T}{\partial y^2} \tag{15}$$

i.e.

$$\frac{\partial T}{\partial t} + w\frac{\partial T}{\partial z} + v\frac{\partial T}{\partial y} = \alpha\frac{\partial^2 T}{\partial y^2} \tag{16}$$

Equation (16) is also a parabolic, second-order partial differential equation, having the same form as the convective–diffusion Equation (2).

Equations 2 and 16 are subject to the following boundary conditions:

(1) a uniform initial concentration and temperature distribution, i.e., at $t = 0$, $C(z, y, 0) = C_0$, and $T(z, y, 0) = T_0$;
(2) a uniform concentration and temperature profile (same as initial values) at the absorber inlet; i.e. at $z = 0$, $C(0, y, t) = C_0$, and $T(0, y, t) = T_0$;
(3) because the tube wall is impermeable, at $y = 0$;

$$\left.\frac{\partial C}{\partial y}\right]_{y=0} = 0 \tag{17}$$

In addition, for nearly isothermal wall conditions, we have, at $y = 0$ $T = T_w$.

Based on the results of a previous one-dimensional (1-D) model (Patnaik et al. 1993), the wall or coolant temperature can be approximated as a linear function of z; i.e., $T_c \approx G_1 z + G_2, G_1 \leq 0$, and G_1 and G_2 depend on the operating conditions (e.g., coolant flow rate) of the absorber.

(4) At the wavy interface; i.e., $y = \delta$, the solution and the vapor are in thermodynamic equilibrium, so that $T_{if} = af(p_v) + b$, $a = a(C_{if})$, $b = b(C_{if})$. Also, an energy balance at the interface yields

$$D_{AB}\frac{\partial C}{\partial y}\dot{i}_{abs} = k\frac{\partial T}{\partial y} \tag{18}$$

where

$$\dot{i}_{abs} = \dot{i}_{r,l} - \dot{i}_r(T_{if}, C_{if}) + \dot{i}_{r,fg}. \tag{19}$$

Equation 18 indicates that the vapor flux relative to the interface is given by molecular diffusion in the liquid immediately adjacent to the interface, any convective effects here being negligible. An explanation follows.

The molar flux of species A is given by (Bird et al. 1960):

$$N_A = -D_{AB}\frac{\partial C_A}{\partial y} + X_A(N_A + N_B) \tag{20}$$

where the second term on the right-hand side represents the convective component of the flux. Hence, we can write:

$$N_A = -D_{AB}\frac{\partial C_A}{\partial y} + X_A(C\,v) \tag{21}$$

where v is the velocity of the fluid relative to the interface. In the case of the smooth laminar film, there is not transverse velocity component relative to the interface other than the small velocity arising from the absorption of liquid. When the interface itself is being displaced inward or outward, because of the passage of waves, the interface velocity caused by absorption is negligible compared to the intrface velocity attributable to waves. In our case, the former is $\sim 10^{-6}$; whereas, the latter is $\sim 10^{-3}$ m/s. Hence, the net flux relative to the moving interface is:

$$N_A = -D_{AB}\frac{\partial C_A}{\partial y} \tag{22}$$

consistent with Equation 18.

Solution and Results

The main difficulty in seeking a numerical solution for Equations 2 and 16 is that the $y = \delta$ boundary of the computational domain is changing with space and time. To overcome this "moving boundary" difficulty, we introduce the normalizing transformation

$$\zeta = y/\delta(z, t) \tag{23}$$

This converts the domain (z, y, t) with a rippled interface $y = \delta$ to a domain (z, ζ, t) with a flat interface $\zeta = 1$.

The parabolic nature of the equations in both space and time called for a marching scheme for the solution. The equations were discretized with backward differencing in space and vertical coordinates and with central differencing along the traverse coordinate, an approach that results in an unconditionally stable scheme. At each vertical location, a tridiagonal coefficient matrix is constructed, in accordance with the second-order nature on each dependent variable. The resulting tridiagonal system using the Thomas algorithm (Pletcher et al 1988), with the dependent variable values at the previous vertical locations and at the present time and also the values at the present location and at the previous time as inputs. The transport equations are interlinked by the boundary conditions, Equations 18 and 19. Convergence of the two solutions was sought at each level, before proceeding to the next one, by solving each matrix in succession. The strong coupling between the two solutions required under relaxation of the equations.

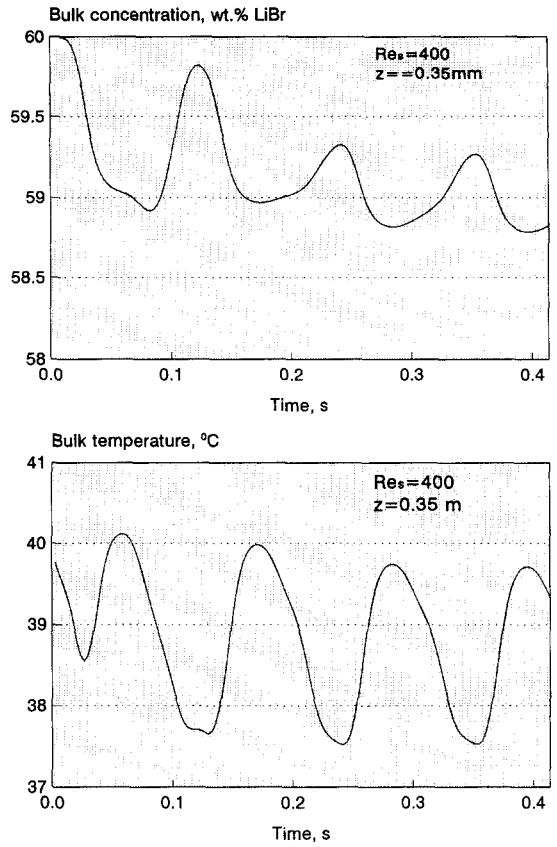

Figure 2 (a) Bulk concentration of abosorbent solution as a function of time. (b) Bulk temperature as a function of time

The assumed operating values are: $T_0 = 40°C$; $T_i = 40°C$; and $T_w = 35°C$; $x_0 = 60\%$ (salt) $= x_i$; and $p_v = 6.4$ mm Hg. The model was first run for the laminar ($Re_s < 20$) and capillary-wave regimes. The governing equations were then solved for a range of Reynolds numbers in the roll-wave regime: 200, 300, 400, 500, and 600.

In Figure 2, the bulk concentration and temperature are plotted as functions of time, at 0.35 m form the top of the absorber tube. As expected with increasing dilution, the fluctuating concentration decays to a periodic steady-state value of 59% (Figure 2a). Heat transfer to the wall cools the solution, causing the mean temperature to decrease (Figure 2b). The temperature fluctuations, however, are out of phase with those of the concentration, because periodically increased absorption liberates heat.

Figure 3 shows the bulk concentration and temperature fluctuating decreasing with distance from the top of the tube at $t = 0.47$ s (periodic steady-state). Over a short tube length of 0.35 m, only two roll waves are present at the given instant, causing the two crests in the bulk concentration and temperature.

The effect of increasing dilution with time is seen by studying the growth of the concentration boundary layer (Figure 4a). At the earliest time shown here ($t = 0.15$ s), the effects of absorption have not yet reached the wall over the length of tube being

studied ($L = 0.35$ m); i.e., in the vicinity of the wall, the concentration is still at its initial value of 60%. At the intermediate time instant of 0.3 s, the boundary layer meets the wall at $z \cong 0.13$ m. This is where the entrance region is separated from the fully developed region at the given instant of time. Finally, at $t = 0.47$ s, the end of the entrance region moves only slightly upstream $z \cong 0.11$ m. Because of the fluctuations in concentration induced by the periodic velocity components, the points where the concentration boundary layer meets the wall fluctuate about a certain mean location. The mean location does not move farther upstream once periodic steady state has been attained (around $t \cong 0.47$ s).

In Figure 4b, the two thermal boundary boundary layers have been plotted, at $t = 0.3$ s. One boundary layer grows from the interface and one from the wall. Growth of these boundary layers follows a path similar to that of the concentration boundary layer, with the oscillating point beyond which the boundary layers are fully developed occurring in the bulk of the film.

The periodic steady-state profiles at various locations along the tube length afford a complementary perspective. Concentration profiles at three different locations from the top are shown in Figure 5a, for $t = 0.47$s. At all three locations, the absorbate has reached the wall, because the concentration here is no longer at its initial value of 60%. Wave-induced inflections are seen in the profiles, particularly nearest to the top of the tube; i.e., at $z = 0.12$ m. At $z = 0.35$ m, the majority of the film has a concentration that is close to the interfacial value. This represents a solution approaching saturation. The different film thicknesses in this figure correspond to different phases of the wave.

The concentration profiles of Figure 5a, in conjunction with the corresponding velocity fields, suggest an explanation to absorption enhancement with waves. The abrupt drop in concentration at the interface corresponding to $z = 0.12$ m and $z = 0.35$ m shows the extent of local dilution there. At these z-locations, the transverse velocity component convects mass and energy toward the wall (inward), with the maximum value of this velocity component occurring at the interface. A coincident peak in the streamwise velocity component (Patnaik 1994) convects downward and mixes the liquid brought in from the interface. On the other hand, at $z = 0.23$ m, a large portion of the film is at almost the same concentration as the interface. This absence of significant gradients, especially near the interface, coincides with an outward transverse velocity component of smaller magnitudes than the component toward the wall. The outward phase spreads over larger sections of the tube and is characterized by low streamwise velocities. Hence, a net transport of mass into the film by the transverse component can be postulated.

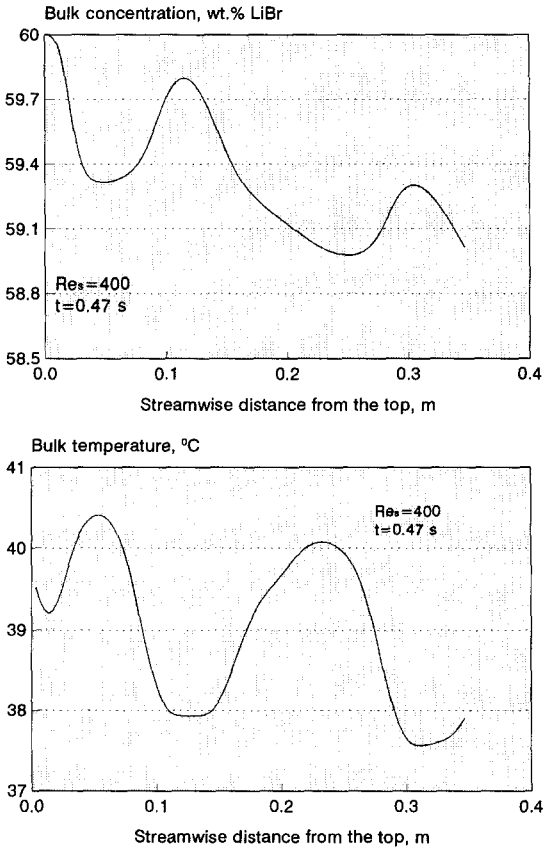

Figure 3 (a) Bulk concentration as function of vertical position. (b) Bulk temperature as function of vertical position

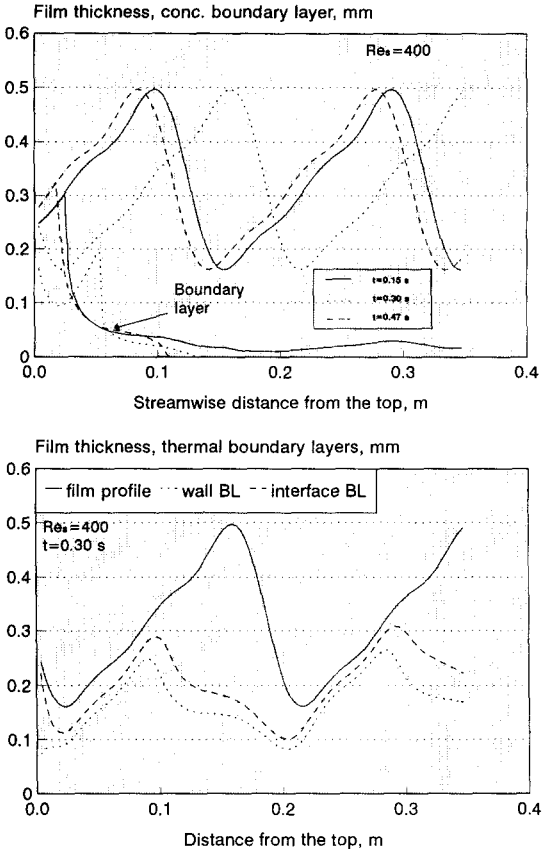

Figure 4 (a) Concentration boundary layer growth with time. (b) Thermal boundary layers versus distance from the top

Temperature profiles at the same times and locations as in Figure 5a are plotted in Figure 5b. Again, at $z = 0.12$ m and $z = 0.35$ m, steep temperature gradients can be observed at the interface, because of the inward normal velocity at these locations, while as much as half of the film cross section is at its saturation temperature at $z = 0.23$ m. All three profiles collapse to the constant wall temperature of 35°C at $y = 0$.

Model validation

To validate the model, the average Sherwood and Nusselt numbers are determined over the species fully-developed section of the absorber (i.e., between $z = 0.11$ m and $z = 0.35$ m, making $L_{FD} = 0.24$ m). This yields the *asymptotic* values of the average coefficients, allowing for comparison, irrespective of absorber

tube/plate length, with corresponding data in the literature. The mass transfer coefficient is calculated as follows:

$$\bar{\kappa} = \frac{\Delta m_{\text{abs}}}{A_{\text{FD}}\rho \text{LMCD}} \tag{24}$$

Consider the numerator:

$$\Delta m_{\text{abs}} = m_{s_i}\frac{(x_{i,\text{FD}} - x_o)}{x_o}$$

$$= \frac{\text{Re}_s(2\pi r_o)\mu}{4}\frac{(x_{i,\text{FD}} - x_o)}{x_o} \tag{25}$$

In the denominator,

$$A_{\text{FD}} = 2\pi r_o L_{\text{FD}} \tag{26}$$

$$\text{LMCD} = \frac{[x_o - x_{\text{eq}}(T_o, p_v)] - [x_{i,\text{FD}} - x_{\text{eq}}(T_{i,\text{FD}}, p_v)]}{\ln\left(\dfrac{x_o - x_{\text{eq}}(T_o, p_v)}{x_{i,\text{FD}} - x_{\text{eq}}(T_{i,\text{FD}}, p_v)}\right)} \tag{27}$$

resulting in the following expression for the Sherwood number:

$$\bar{\text{Sh}} = \frac{\bar{\delta}\text{Re}_s\text{Sc}(x_{i,\text{FD}} - x_o)}{4L_{\text{FD}}x_o\text{LMCD}} \tag{28}$$

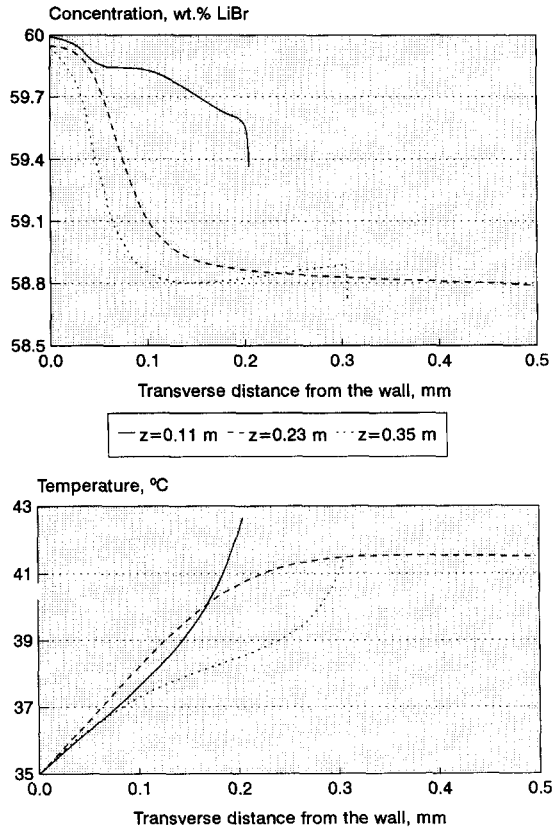

Figure 5 (a) Concentration profiles at different positions along the tube; $\text{Re}_s = 400$, $t = 0.47$ s; ——— $z = 0.11$ m; ----- $z = 0.23$ m; ····· $z = 0.35$ m. (b) Temperature profiles at different positions along the tube; $\text{Re}_s = 400$, $t = 0.47$ s; ——— $z = 0.11$ m; ----- $z = 0.23$ m; ····· $z = 0.35$ m

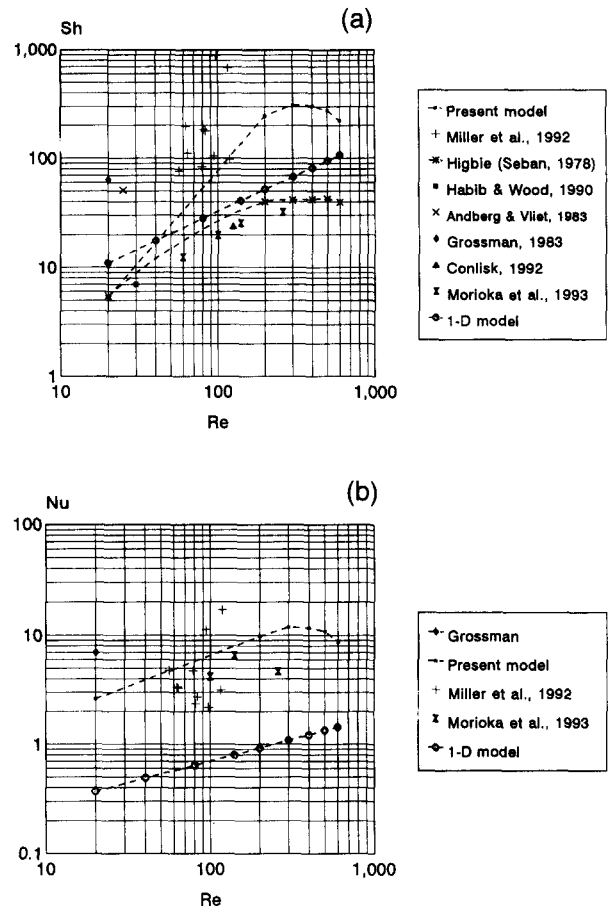

Figure 6 (a) Average Sherwood numbers as functions of Reynolds numbers. (b) Average heat transfer coefficients as functions of Reynolds numbers

where the entering LiBr solution Schmidt number for the given operating conditions is 4145 (Uemura and Hasaba 1964).

Similarly, assuming the absorber heat load to be given by:

$$q = m_{s_i}c_{p_s}(T_i - T_o) + \Delta m_s i_{\text{abs}} \tag{29}$$

the average wall Nusselt number can be derived to be:

$$\bar{\text{Nu}} = \frac{\bar{\delta}\text{Re}_s\text{Pr}\left[(T_{i,\text{FD}} - T_o) + \left(\dfrac{x_{i,\text{FD}} - x_o}{x_o}\right)\dfrac{i_{\text{abs}}}{c_{p_s}}\right]}{4L_{\text{FD}}\text{LMTD}} \tag{30}$$

where

$$\text{LMTD} \equiv \frac{(T_o - T_w) - (T_{i,\text{FD}} - T_w)}{\ln\left(\dfrac{T_o - T_w}{T_{i,\text{FD}} - T_w}\right)} \tag{31}$$

and the entering solution Prandtl number is 27 (Uemura and Hasaba 1964).

The transport coefficients were calculated for the smooth film at $\text{Re}_s = 20$, and for varying Re_s in the roll wave regime. They were then compared to experimental and theoretical data in the literature for other vertical-tube or -plate absorbers in similar applications.

The average Sherwood number is plotted in Figure 6a versus the film Reynolds number. There is good agreement between the model prediction and Higbie's penetration theory (Seban 1978)

for the smooth film ($Re_s = 20$); the model yields a value of 5.34, while Higbie's theory predicts 5.45. It should be noted that the latter was developed for isothermal mass transfer. At the same Re_s, the models of Grossman (1983) and Andberg and Vliet (1983) predict larger Sh numbers, by a factor of 10. Discrepancies in the calculation of the entrance region may explain these differences, for the fully developed values show better agreement. A composite correlation used by the 1-D model developed by Patnaik et al. (1993) yields a Sherwood number of 10.98, nearly twice the Higbie theory value. Inclusion of the entrance region in the calculation could explain this discrepancy. For Reynolds numbers in the wavy regime, the 1-D model Sherwood numbers are intermediate between those predicted by Higbie's theory and the 2-D model. A noteworthy feature of the 2-D model is that the mass transfer coefficient reaches a maximum value in the roll wave regime (at $Re_S \cong 300$). It is hypothesized that the Sherwood number starts to decrease for higher Reynolds numbers, because the decreasing wave frequencies (Brauner 1989) yield incomplete waves over the given tube length. Increasing the flow further would not yield savings in the absorption area, for constant mass absorbed.

Habib and Wood (1990) assumed a smooth film even at a Reynolds number of 30, and predict a Sherwood number slightly below Higbie's value. Experimental data were found to be available primarily for the higher side of the capillary wave regime. Results from Higbie's theory and Conlisk's analytical model (1992) are in close agreement with the data of Morioka et al. (1993), but the data of Miller et al. (1992) in this regime yield much higher mass transfer coefficients. Although unexpected at low Reynolds numbers, roll waves were detected and can explain the unusually high values of the Sherwood numbers. The present model predictions for roll waves are compatible with the values detected by Miller et al., although at different Re numbers.

Heat transfer to the wall (Figure 6b) shows that variations in the average Nusselt number are not as marked as those in the Sherwood number. Again, the model seems to overpredict the data of Morioka et al. (1993). The scatter of the data of Miller et al. (1992) precludes a close comparison and underlines the difficulties associated with the transition regime. However, the range of the measured Nusselt numbers is consistent with the predictions of the present model. The Nusslet number peaks at Reynolds numbers in the order of 200, suggesting that increased film thicknesses tend to increase the resistance to heat transfer.

Conclusions

Waves in falling films enhance absorption over the rates predicted by smooth-film theories. To model this complex combined heat and mass transfer process, approximate roll wave hydrodynamics was derived in previous work. The hydrodynamics was used here in the energy and species balance equations, coupled nonlinearly at the vapor–liquid interface. Simultaneous heat and mass transfer enhancement attributable to roll waves is difficult to model because of instabilities inherent to the transitional regime. The model was run for low Reynolds numbers corresponding to the laminar film case and for the roll wave regime. Calculated average heat and mass transfer coefficients are comparable to those found in the literature at low Reynolds numbers. At high Reynolds numbers, the dimensionless coefficients are still a good approximation, but the Reynolds number ranges do not agree well with experimental values.

This work broadens our understanding of the complex phenomenon of wavy film absorption, and provides a model that can calculate enhancement. The enhancement associated with roll waves is considerable: Sherwood numbers in the order of 300 are possible; whereas, smooth film measured and calculated values range from 30 to 80 for the same regime. The enhancement appears to be a strong function of the wave hydrodynamics: the velocity component normal to the interface and the downward velocity are approximately in phase so as to maximize transport into the film. Clearly, the inclusion of other frequencies in the model could shift the relative phase between the velocity components, but no other dominant frequencies were consistently observed during the study leading to the hydrodynamics formulation. Hence, the explanation for the observed enhancement offered in the present work is plausible.

References

Andberg, J. W. and Vliet, G. C. 1983. Design guidelines for water–lithium bromide absorbers. *ASHRAE Trans.*, **89**, 220–232

Beschkov, V. and Boyadjiev, C. 1983. Numerical investigation of gas absorption in a wavy film flow. *Chem. Eng. Communication*, **20**, 173–182

Bird, R. B., Stewart, W. E. and Lightfoot, E. N. 1960. *Transport Phenomena*, Wiley, New York, Part III

Brauner, N. 1989. Modeling of wavy flow in turbulent free falling films. *Int. J. Multiphase Flow*, **15**, 505–520

Grigor'eva, N. I. and Nakoryakov, V. E. 1977. Exact solution of combined heat- and mass-transfer problem during film absorption. *Inzh.-Fiz. Zh.* (U.S.S.R.), **33**, 893–898

Grossman, G. 1983. Simultaneous heat and mass transfer in film absorption under laminar flow. *Int. J. Heat Mass Transfer*, **26**, 357–371

Grossman, G. and Heath, M. T. 1984. Simultaneous heat and mass transfer in absorption of gases in turbulent liquid films. *Int. J. Heat Mass Transfer*, **27**, 2365–2376

Habib, H. M. and Wood, B. D. 1990. Simultaneous heat and mass transfer for a falling film absorber — The two-phase flow problem. Paper presented at the 12th annual ASME International Solar Energy Conference, Solar Engineering 1990 (pp. 61–67) Miami, FL, USA

McNeely, L. 1979. Thermodynamic properties of aqueous solutions of lithium bromide. *ASHRAE Trans.*, **85**, 413–434

Miller, W. A., Perez-Blanco, H. and Patnaik, V. 1992. *Advanced surfaces for vertical tube absorbers*. Final report to the Gas Research Institute (Contract # 5089-243-1844)

Marioka, I., Kiyota, M. and Nakao, R. 1993. Absorption of water vapor into a film of aqueous solution of LiBr falling along a vertical pipe. *JSME Int. J.*, **36**, 351–356

Patankar, S. V. 1988. Elliptic systems: Finite-difference method I. In *Handbook of Numerical Heat Transfer*, W. J. Minkowycz, E. M. Sparrow, G. E. Schneider and R. H. Pletcher (eds.), Wiley, New York, 215–40

Patnaik, V. (1994). Combined heat and mass transfer in wavy film absorption. Ph.D. thesis, The Pennsylvania State University, University Park, PA, USA

Patnaik, V., Perez-Blanco, H. and Ryan, W. A. 1993. A simple model for the design of vertical tube absorbers. *ASHRAE Trans.* **99**

Penev, V., Krylov, V. S., Boyadjiev, C. and Vorotilin, V. P. 1972. Wavy flow of thin liquid films. *Int. J. Heat Mass Transfer*, **15**, 1395–1406

Pletcher, R. H., Minkowycz, W. J. Sparrow, E. M. and Schneider, G. E. 1988. Overview of basic numerical methods. In *Handbook of Numerical Heat Transfer*, W. J. Minkowycz, E. M. Sparrow, G. E. Schneider and R. H. Pletcher (eds.), Wiley, New York, 52–78

Seban, R. A. 1978. Transport to falling films, *Int. Heat Transfer Conference*, Hemisphere (Bristol, PA) 417–428

Uemura, T. and Hasaba, S. 1964. Studies on the lithium bromide–water absorption refrigerating machine. *Technol. Report of Kansai Univ.* **6**, 31–55

van der Wekken, B. J., Wassenaar, R. H. and Segal, A. 1988. Finite element method solution of simultaneous two-dimensional heat and mass transfer in laminar film flow. *Waerme- und, Stoffuebertragung*, **22**, 347–354

Wasden, F. K. and Dukler, A. E. 1990. A numerical study of mass transfer in free falling wavy films. *AIChE J.* **36**, 1379–1390